energies

MDPI

Article

Study on Superconducting Magnetic Energy Storage for Large Subway Stations with Multiple Lines

Wenjing Mo [1], Boyang Shen [1,*], Xiaoyuan Chen [2,*], Yu Chen [1] and Lin Fu [1,*]

[1] College of Transportation, Tongji University, Shanghai 201804, China
[2] School of Engineering, Sichuan Normal University, Chengdu 610101, China
* Correspondence: shenboyang@tongji.edu.cn (B.S.); chenxy@sicnu.edu.cn (X.C.); linfu@tongji.edu.cn (L.F.)

Abstract

With accelerating urbanization, subway stations, as high-energy-consumption sectors, face significant challenges in maintaining power supply stability and ensuring power quality. This paper proposed a novel voltage compensation solution utilizing superconducting magnetic energy storage (SMES) to suppress voltage fluctuations in the traction system of a large subway station with multiple lines, which was caused by frequent acceleration and regenerative braking of multiple subway trains. Using the MATLAB/Simulink platform, a model of the traction power system with SMES for a large subway station with multiple lines was constructed. Appropriate control methods and hierarchical control strategies were used to suppress voltage fluctuations in both single-line and multi-line configurations at subway stations. The technical advantages of SMES in rapid response and efficient charging/discharging were explored. Overall, results show SMES with the novel control strategies can effectively suppress voltage fluctuations on both single- and triple-line configurations, validating the feasibility in mitigating voltage fluctuations and enhancing regenerative braking energy utilization.

Keywords: superconducting magnetic energy storage (SMES); subway station traction system; voltage fluctuation suppression

check for updates

Academic Editor: Ryszard Palka

Received: 27 September 2025
Revised: 19 October 2025
Accepted: 20 October 2025
Published: 24 October 2025

Citation: Mo, W.; Shen, B.; Chen, X.; Chen, Y.; Fu, L. Study on Superconducting Magnetic Energy Storage for Large Subway Stations with Multiple Lines. *Energies* **2025**, *18*, 5596. https://doi.org/10.3390/en18215596

Copyright: © 2025 by the authors. Licensee MDPI, Basel, Switzerland. This article is an open access article distributed under the terms and conditions of the Creative Commons Attribution (CC BY) license (https://creativecommons.org/licenses/by/4.0/).

1. Introduction

In response to the global call for low carbon, renewable energy has been widely promoted and used [1,2]. However, renewable energy has the characteristics of intermittent and random output power, leading to poor power quality when integrated into the grid. In recent years, the application of SMES in renewable energy integration has become increasingly prominent [3–5]. Similar to the issues above, global subway transportation also suffers problems of power fluctuations and power qualities in the tractions supply systems, which could possibly be solved by SMES's superior capability of smoothing power fluctuations, absorbing grid shocks, and improving grid stability [6–8].

Since the first attempt in 1970s, SMES devices started to connect to the power grid compensate for power fluctuations and oscillations, improving grid power supply stability [9–12]. A 1 MJ SMES device and A 5 MJ SMES device were built to enhancing power system stability [13–15]. A 3 MJ/750 kVA SMES device was experimentally tested, and the system could effectively protect sensitive power loads during sudden disruptions or voltage drops [16]. A large-capacity SMES device was successfully developed and connected to the power grid, with a response time of less than 10 ms, verifying the system's ability to suppress active power oscillations and improve power quality [17,18].

SMES has been used to improve grid quality in various high-speed transportation systems around the world, such as Japan's Shinkansen, France's TGV, and Germany's ICE. These systems have a characteristic of pulsating power demand, where the peak power requirement of a single train can exceed 10 megawatts, necessitating a very large storage capacity for SMES [19]. Refs. [20–22] proposed hybrid energy storage solutions that combines the advantages of energy-oriented storage and power-oriented storage, which covers superconducting technologies and other types of energy storage technologies. Energy-oriented storage has a higher energy density with lower power density, while power-oriented storage has a lower energy density but higher power density. Batteries can be used for long-term fluctuations, while superconducting storage can handle short-term fluctuations. To improve the energy utilization of SMES under multiple distribution conditions and reduce storage costs, ref. [23] suggested sharing a single SMES coil among several circuit branches to meet the independent energy exchange requirements.

In urban subway rail transit, when the subway trains are in regenerative braking mode, a large amount of braking energy is generated. Only a small portion of this braking energy is absorbed by adjacent vehicles in traction mode, while the majority will be fed back into the traction system, causing an increase in network voltage. If the voltage exceeds the maximum limit, regenerative braking failure can occur, posing a safety risk [24,25]. To address this issue, ref. [26] adopted a ground-based supercapacitor energy storage system to recover the regenerative braking energy of trains. Ref. [27] analyzed the impact of different voltage fluctuation ranges on subway equipment in detail and suggested using voltage fluctuation resistance devices to mitigate voltage fluctuation effects on subway operation, ensuring safe and stable operation of the subway system. To resolve issues such as sudden stops of elevators due to voltage fluctuations in elevator systems, ref. [28] proposed a 400 V voltage fluctuation-resistant emergency power supply system for subway elevators. This research method mainly utilizes a combination of batteries and supercapacitors for emergency energy storage supply. Using energy storage technology to solve voltage fluctuation problems is the most effective approach [29]. There are many factors that cause voltage and power fluctuations in the grid system, and the train loads in rail transit also exhibit strong volatility, which makes the power sources and loads in the electric power system containing rail transit both highly volatile and uncertain [24,30,31]. Currently, SMES application in urban rail transit is still at the stage of principle analysis and feasibility assessment. Refs. [32,33] address energy issues in railway transportation and propose an energy compensation scheme for a superconducting energy storage system, with results indicating that SMES effectively mitigates voltage sags and maintains voltage stability.

However, to the best of our knowledge, the studies on using SMES to compensate for the fluctuations of the traction power system particularly for multiple lines in a large subway station are missing. This study proposed a novel superconducting energy storage method to be used in a large subway station with multiple lines, addressing voltage fluctuations. It technically evaluates the effectiveness of suppressing voltage fluctuations and improving the utilization of regenerative braking energy.

2. SMES for a Large Subway Station with Multiple Lines

A new framework for a large subway station with multiple lines, and its traction system with SMES is shown in Figure 1.

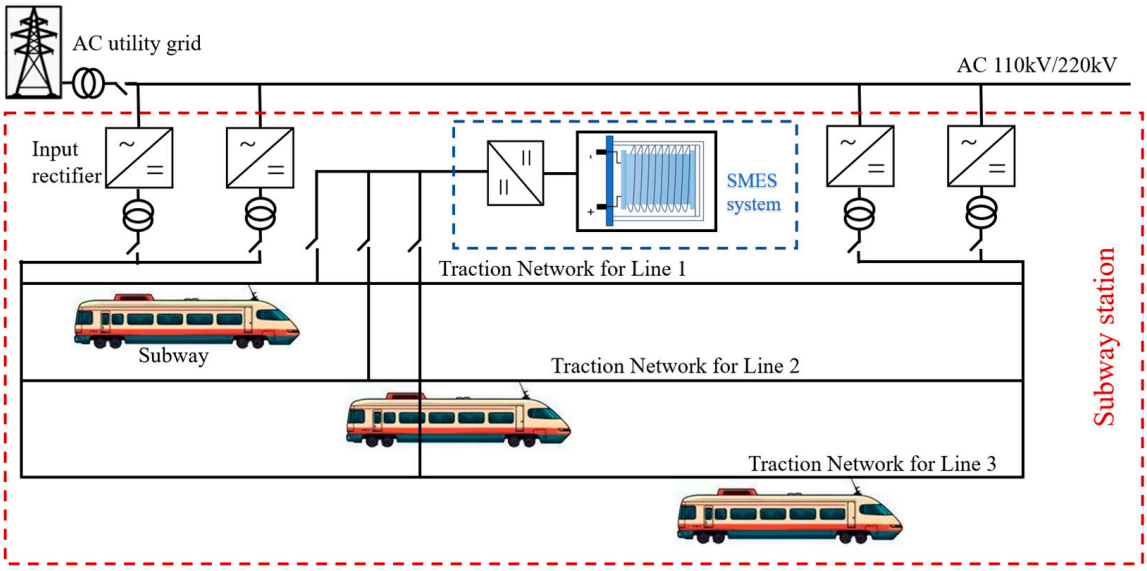

Figure 1. A new framework: a large subway station with multiple lines, and its traction system with SMES.

Traction energy constitutes the largest portion of total energy usage in subway systems. The study shows that traction energy consumption accounted for 43%, while ventilation and air conditioning accounted for 35% [34]. Influenced by factors such as train frequency, operating mileage, passenger volume, train formation, and vehicle weight, traction energy consumption exhibits significant fluctuations throughout the day, peaking during morning and evening rush hours. Urban rail transit primarily experiences two peak periods: morning and evening commutes, during which passenger volume and train frequency exceed other times. The traction energy consumption dataset recorded on a typical subway line in China in March 2019 is shown in Figure 2 [35].

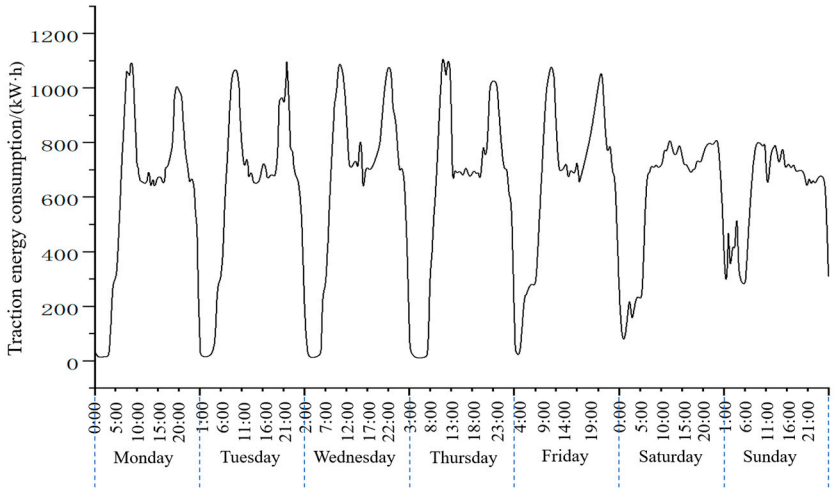

Figure 2. Traction energy of a typical subway line (replot from [35]).

Subway station power supply systems employ zone-based distribution, simultaneously providing AC power (for station equipment) and DC power (for train traction). These power types were allocated through distinct substations and distribution systems. In urban rail transit traction power supply systems, the distribution of traction substations must consider both line length and power capacity requirements. Some smaller stations lack on-site traction power systems, relying instead on cables from nearby substations to supply trains. In larger stations, traction substations were typically located at station ends or in

underground equipment levels, isolated from the track area. Urban high-voltage power is rectified at traction substations into 750 V/1500 V DC. This DC power is extended via cables or rigid contact lines to the platform track area, ensuring a continuous supply [36].

For urban rail transit DC traction power supply systems, the traction system experiences voltage fluctuations influenced by various factors. Changes in train operating states constitute the primary cause of voltage fluctuations in the traction system. Especially in subway system, a large number of trains frequently accelerate and brake. During acceleration, the traction motors on the train absorb significant electrical energy from the traction system, where this flow of energy through the feeder lines and overhead contact system to the train causes noticeable voltage drops in the DC traction system. When trains operate in regenerative braking mode, traction motors switch to generator operation, converting kinetic energy into electrical energy fed back into the DC traction system, where this causes voltage rise in the DC network. Furthermore, since uncontrolled rectifier devices using diodes are widely employed, the electrical energy generated during regenerative braking cannot be directly fed back into the AC grid. These two types of voltage fluctuations significantly impact the stability and power quality of the supply system [37].

Large subway stations face significant load variability issues. During morning and evening rush hours, frequent train starts, stops, accelerations, and braking caused instantaneous power surges, triggering frequent drops or sudden spikes in DC bus voltage. For DC systems, based on DC fault characteristics, when a DC power system fails, the DC voltage changes extremely rapidly. The fault current may be several times greater than the rated current, damaging fragile converters and causing generators to shut down [38]. Consequently, China imposed specific requirements on voltage fluctuations within urban rail transit traction systems. According to the national standard "Railway Transportation-Traction Power Supply System Voltage" (GB/T 1402-2010 [39]), China's urban rail transit systems primarily utilize two DC voltage levels: 750 V and 1500 V. For 1500 V DC power supply systems, normal operating voltage fluctuations are permitted within the range of 1000–1950 V, with specific restrictions on duration. Voltage dropping to 1000 V must not exceed 2 min. When voltage rises to the 1800–1950 V range, duration should be limited to 5 min or less, with subsequent operation requiring voltage to return below 1800 V. Only under non-sustained conditions, such as regenerative braking, may the voltage operate between 1800 V and 1950 V [39]. Elevated voltages risk damaging traction substation rectifier units or onboard train electrical equipment, posing safety hazards. Furthermore, voltage instability reduces traction motor efficiency, increasing energy consumption and undermining energy conservation and environmental protection goals.

SMES systems exhibit zero resistance at critical temperatures, significantly reducing energy losses compared to other storage methods. Their exceptionally high-power density and millisecond-level rapid response enable highly efficient energy storage and release, capable of matching the transient power fluctuations during frequent starts and stops of subway trains. Using superconducting energy storage devices can address fluctuations in subway stations characterized by small amplitude, short duration, and high frequency. Compared to battery storage, the materials used in superconducting energy storage devices are virtually non-toxic, eliminating environmental pollution concerns. When contrasted with supercapacitor storage, superconducting energy storage devices are more compact, saving significant space. Thus, superconducting energy storage technology offers distinct performance advantages for large subway stations, fulfilling the ideal energy storage requirements of metro power supply systems. By stabilizing DC traction system voltage and absorbing regenerative energy, superconducting storage systems not only enhance power supply quality but also significantly reduce overall system energy consumption.

3. SMES Voltage Compensation Principle

To enable bidirectional energy flow, the superconducting energy storage system charges the superconducting coil to store energy when the traction system voltage rises, thereby lowering the traction system voltage to its nominal value. When the traction system voltage drops, the superconducting coil discharges to release energy, raising the traction system voltage back to its nominal value. Simple boost or buck circuits cannot achieve this functionality. Therefore, a DC/DC converter specifically designed for superconducting energy storage systems employs the H-bridge chopper principle. This enables voltage boosting/buckling, polarity reversal, and four-quadrant operation, facilitating bidirectional energy flow. The H-bridge consists of four switching transistors. By varying the switching combinations, it can output positive voltage, negative voltage, positive current, and negative current to achieve four-quadrant operation. This paper employs switching devices composed of two IGBTs and diodes, along with two additional diodes. The DC/DC converter plays a crucial role in energy storage systems, primarily enabling bidirectional energy flow and efficient management. It flexibly converts electrical energy between storage devices—such as batteries, supercapacitors, and superconducting magnets—and the DC bus (or load) according to system requirements. The DC/DC conversion circuit in this paper connects its input to a 1500 V DC traction system. The freewheeling diodes are configured with the same voltage rating as the IGBT. A voltage-stabilizing capacitor C is paralleled on the DC side to smooth voltage transients during normal operation. Its sufficiently large capacitance maintains a stable voltage without significant fluctuations during continuous charging and discharging, promoting stable SMES operation. A superconducting coil compensates for voltage fluctuations during sudden surges and dips. During MATLAB/Simulink simulation modeling, power device parameters retain their default software settings.

The DC/DC converter operates in three fundamental modes: charging mode, discharging mode, and constant current mode [40], as shown in Figure 3.

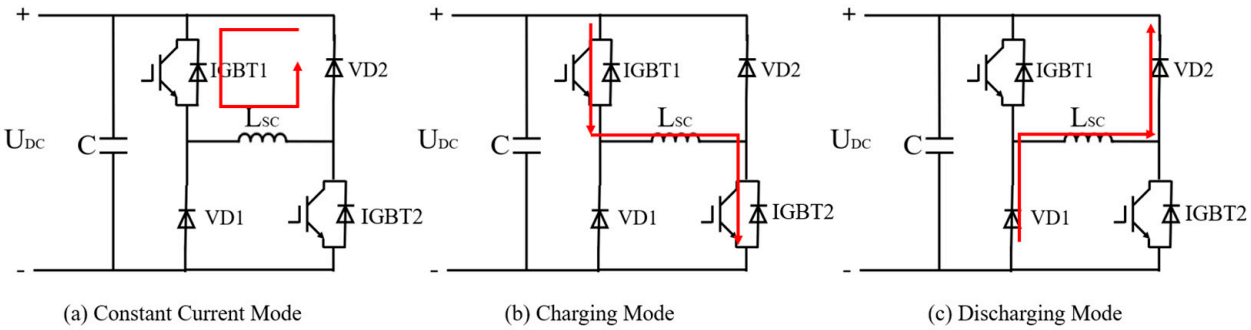

Figure 3. Schematics of SMES operation in different modes.

(1) IGBT1 and VD2 are conducting, while IGBT2 and VD1 are off. The freewheeling current (i_{sc}) forms a circulating loop through IGBT1—L_{sc}—VD2. When switching device losses are neglected, i_{sc} remains constant, and the energy stored in L_{sc} remains unchanged. At this point, the DC/DC converter operates in freewheeling mode.

(2) IGBT1 and IGBT2 are both on, while VD1 and VD2 are off. The system charges L_{sc} through the path IGBT1—L_{sc}—IGBT2. When switching device losses are negligible, i_{sc} increases, and the energy stored in L_{sc} rises. At this point, the DC/DC converter operates in charge mode.

(3) IGBT1 and IGBT2 turn off simultaneously, while VD1 and VD2 turn on. L_{sc} discharges energy through the path VD1—L_{sc}—VD2—C, then through the converter to the

system. The current i_{sc} decreases, and the energy stored in L_{sc} decreases. At this point, the DC/DC converter operates in a discharge state.

During charging, the SMES coil absorbs excess energy from the external DC line. According to Kirchhoff's voltage and current laws, the current and voltage equations can be expressed as:

$$L_{sc}\frac{di_{sc}}{dt} = -R_{sc}i_{sc} + u \tag{1}$$

$$C\frac{du}{dt} = i_{dc} - i_{sc} \tag{2}$$

where L_{sc}, i_{sc}, and R_{sc} represent the inductance, current, and resistance of the superconducting energy storage magnet, respectively; C denotes the DC-side capacitance; u denotes the DC-side voltage; i_{dc} denotes the DC-side current.

During transient and steady-state storage conditions, the transient SMES current remains nearly constant when switching losses are neglected. Considering the equivalent loss resistance R_{sc} in series with the SMES coil, the transient current and voltage equations can be expressed as in Equations (3) and (4):

$$L_{sc}\frac{di_{sc}}{dt} = -R_{sc}i_{sc} \tag{3}$$

$$C\frac{du}{dt} = i_{dc} \tag{4}$$

During discharge, the SMES coil compensates for the energy deficiency in the external DC line. According to Kirchhoff's voltage law and Kirchhoff's current law, the current and voltage equations can be expressed as:

$$L_{sc}\frac{di_{sc}}{dt} = -R_{sc}i_{sc} - u \tag{5}$$

$$C\frac{du}{dt} = i_{dc} + i_{sc} \tag{6}$$

Assuming the duty cycle of the switching operation is D, Equations (1)–(4) can be combined to form the integrated state equation for the charging storage mode:

$$L_{sc}\frac{di_{sc}}{dt} = -R_{sc}i_{sc} + Du \tag{7}$$

$$C\frac{du}{dt} = i_{dc} - Di_{sc} \tag{8}$$

where D denotes the duty cycle of the switching device.

Given the identical energy storage equation and duty cycle D in Equations (7) and (8), Equations (3)–(6) can be combined to form the comprehensive state equation for the discharge storage mode:

$$L_{sc}\frac{di_{sc}}{dt} = -R_{sc}i_{sc} - (1-D)u \tag{9}$$

$$C\frac{du}{dt} = i_{dc} + (1-D)i_{sc} \tag{10}$$

Equations (7) and (8) describe the relationships among parameters during the SMES charging state; Equations (9) and (10) describe the relationships among parameters during the SMES discharging state.

The voltage control of this system, combined with the superconducting energy storage device designed in this paper, enables efficient energy storage and release in the superconducting coil. In MATLAB/Simulink, integrating the PWM module with a PI controller is an effective method for controlling DC/DC converters. The PI controller generates the duty

cycle for the PWM signal, which is then converted into the actual PWM signal to drive the switching of devices such as MOSFETs and IGBTs. The integration of the DC/DC converter with the PI controller and PWM modulation technology enables efficient energy management and precise control. The PI controller regulates the traction system voltage, ensuring rapid system response and stable operation. PWM modulation, by adjusting the switching device duty cycle in conjunction with the DC/DC converter, facilitates bidirectional energy flow. It controls the switching of the converter's devices, thereby supporting both charging and discharging of the energy storage device.

The DC/DC converter control system designed in this study employs a dual-switch cooperative strategy based on PI control. By regulating the operating states of switching devices IGBT1 and IGBT2, it enables three-mode operation of the superconducting energy storage system: When traction system voltage exceeds the 1500 V nominal value, the control system simultaneously turns on IGBT1 and IGBT2, placing the superconducting energy storage system into charging mode. When the voltage falls below the 1500 V nominal value, IGBT1 and IGBT2 are simultaneously turned off, switching the system to discharge mode; when one switch is on and the other is off, the system maintains its energy storage state. To implement this control strategy, the system employs a closed-loop control method based on PI regulation. The actual detected voltage is normalized to the same dimensional scale as the setpoint using a gain of 1/1500. This normalized deviation serves as the control signal input to the PI controller. The output signal from the PI controller is then compared with a triangular carrier wave of 1 kHz frequency and with an amplitude range of [0, 1]. Due to the triangular wave's amplitude range, the PI controller's output signal is offset by 0.5 before comparison to generate the final PWM control signal. This control scheme aims to effectively smooth fluctuations in the traction system voltage while achieving efficient recovery of regenerative braking energy.

4. Simulation and Analysis of Superconducting Energy Storage Devices

4.1. Simulation Environment

This paper employed the MATLAB/Simulink platform as the simulation environment. Circuit components were accessed from module libraries, with some algorithm programming integrated using MATLAB Function blocks. System simulation was achieved through a combination of interactive modeling and programming.

4.2. Single-Line Study

In actual subway station operations, multiple trains running simultaneously cause complex voltage fluctuations in the traction system. This paper employed a simplified voltage step method to simulate train-induced voltage variations in the traction system, representing a relatively coarse approximation. For trains, a more accurate modeling approach involves directly modeling their traction drive systems, including key components such as inverters and motors. Some papers treat this as a current source model. To simplify analysis, this paper sets the following simulation conditions: only three trains operating simultaneously on a single line were considered, and one SMES device was configured in the subway station power supply system. Analysis of traction system voltage fluctuations will be conducted under the following three scenarios: first, when train regenerative braking causes an increase in traction system voltage; second, when train acceleration causes a decrease in traction system voltage; Third, the phase where the traction system voltage remains relatively constant during steady-state train operation. In actual operation, the amplitude and duration of voltage fluctuations caused by each train vary. To simplify the experiment, each fluctuation was uniformly set to $\pm$100 V. The simulation models a voltage increase of 100 V caused by the regenerative braking of each train and a voltage

decrease of 100 V caused by the acceleration start of each train. The train's regenerative braking/acceleration startup simulated voltage fluctuations through abrupt changes in resistance.

4.2.1. Different Scenarios of Single-Line Operation

Based on the aforementioned DC/DC conversion circuit and control system design, a complete circuit and control system simulation model was constructed in the MATLAB/Simulink platform. Comparative simulations were conducted under conditions with and without the superconducting energy storage device (SMES) connected, by varying the traction system voltage. During the simulation, various voltage variation scenarios were set, such as the time and magnitude of voltage rise or fall. The simulation results were analyzed to evaluate the SMES device's suppression effect on traction system voltage fluctuations and assess its operational performance. Table 1 shows the parameters of traction system and SMES.

Table 1. Parameters of traction system and SMES.

Item	Parameters	Value
Traction system	DC voltage	1500 V
	Current	1000 A
	Power	1500 KW
SMES	Inductance	1 H
	Operating current	500 A
	Energy storage	125 KJ

Considering this study was solely a verification simulation experiment, the simulation duration was set to 3 s.

This study verified the voltage fluctuation suppression effect of superconducting energy storage devices on traction systems through comparative simulation analysis. The subsequent simulation results presented voltage waveform variations with and without SMES integration. By adjusting key parameters such as the amplitude and duration of voltage fluctuations, as well as the initial current of the energy storage magnets, the system comprehensively examines the dynamic response characteristics and voltage stabilization performance of SMES under various operating conditions. This enables a thorough evaluation of its contribution to enhancing grid stability during actual operation.

(1) Simulation Results for Traction system voltage increase

In this simulation, the initial current of the energy storage magnet was set to 300 A.

Scenario ①: Traction system voltage rose to 1600 V.

Train Condition: One train in regenerative braking mode, two trains in constant-speed operation (as shown in Figure 4).

Analysis of simulation results in Figure 4 revealed that for a single-track system without superconducting energy storage devices, when one train undergoes regenerative braking at the 1 s mark while the other two trains maintain constant speed, the traction system voltage rose to 1600 V and remained elevated for approximately 1 s. After installing the superconducting energy storage system (SMES), its rapid response capability immediately smooths voltage fluctuations. Under the current configuration, the SMES capacity sufficiently covered voltage spikes reaching 1600 V. However, if braking energy increases further (e.g., multiple trains braking simultaneously), it required further verification whether the initial current of the SMES needs to be increased to ensure its smoothing capacity can meet the demands of larger power fluctuations.

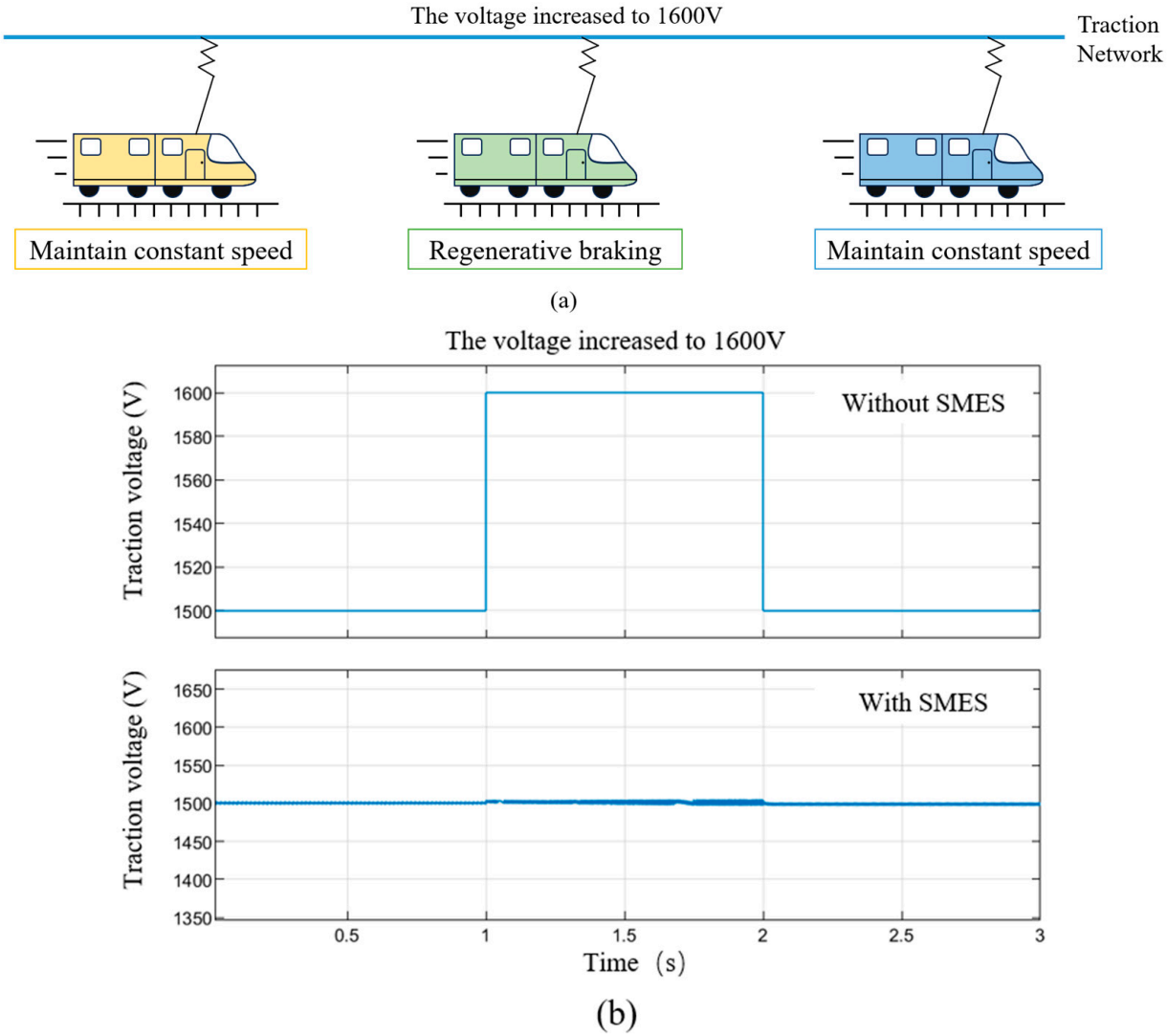

Figure 4. Scenario ①: (**a**) train operating condition, (**b**) with SMES vs. without SMES.

(2) Simulation Results for Traction system Voltage Decrease

In this simulation section, the initial current of the energy storage magnet was set to 400 A.

Scenario ②: Traction system voltage dropped to 1400 V.

Train condition: One train is in acceleration start mode, while the other two trains are in constant-speed operation, as shown in Figure 5.

Analysis of simulation results in Figure 5 revealed that when one train accelerates from a start while the other two maintain constant speed, the traction system voltage dropped to 1400 V and remained at this level for approximately 0.5 s. After configuring the SMES system, with the initial current of the energy storage magnet set to 400 A in the simulation, the SMES responds rapidly, quickly restoring the voltage to the nominal value of 1500 V. However, capacity or response speed bottlenecks persisted under low-voltage conditions, preventing complete suppression of subsequent minor fluctuations. Further increasing the initial storage magnet current to 500 A in the simulation enabled the SMES to effectively prevent deep voltage dips, enhancing traction system power quality during train start-up conditions and demonstrating the SMES system's ultra-fast dynamic response capability.

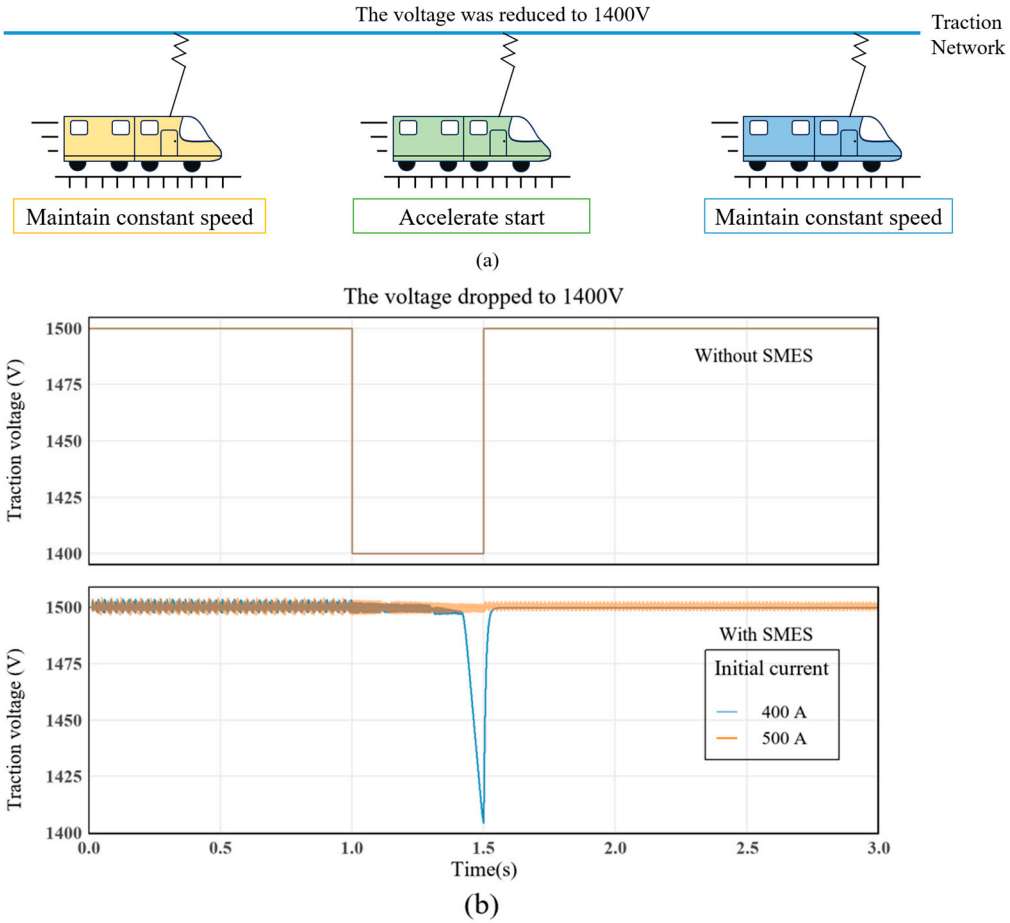

Figure 5. Scenario ②: (**a**) train operating condition, (**b**) with SMES vs. without SMES, and the SMES with an initial current of 400 A and 500 A.

4.2.2. Analysis

In the simulation analysis of voltage rise scenarios, the case of a 1600 V voltage increase was specifically examined. Under these conditions, the SMES demonstrated rapid response capabilities and effectively mitigated voltage fluctuations. Notably, the 1600 V fluctuation was completely suppressed, thereby preventing potential equipment risks associated with overvoltage. Furthermore, simulation results indicate near-instantaneous recovery at 1600 V, with the SMES capacity at an initial current of 300 A already sufficient to meet suppression requirements. When facing higher braking energy demands (e.g., simultaneous braking of multiple trains), enhancing the system's energy throughput capacity and suppression effectiveness through increased initial current or optimized control strategies is necessary to ensure the safe and stable operation of the traction power supply system.

Simulation analysis under voltage reduction scenarios demonstrated the SMES's excellent response characteristics during traction system voltage dips. For instance, at 1400 V, an SMES with an initial current of 400 A rapidly responds and restores voltage to the 1500 V nominal value, though minor subsequent fluctuations occur. When the initial current was increased to 500 A, the system completely avoids the risk of deep voltage dips. SMES enhanced voltage stability. These simulation results validated SMES's capability to improve power quality during train start-up conditions. They also indicated that increasing the initial current of the energy storage magnets effectively enhances the system's suppression capability against voltage dips. However, for extreme operating conditions, further optimization of capacity configuration or control strategies is still required to achieve complete suppression.

4.3. Multi-Line Study

Given the complex operating conditions of multiple parallel lines in subway stations, the previously completed simulation of the superconducting energy storage system was validated only for single-line scenarios. The rapid response characteristics of superconducting energy storage are advantageous for suppressing transient voltage and power fluctuations. While other energy storage methods can achieve similar suppression, they exhibit slower response times compared to SMES. However, SMES coils are significantly more expensive than traditional battery storage. For large subway stations with multiple parallel lines, to enhance energy utilization efficiency under multi-line distribution conditions and reduce energy storage costs, we propose sharing a single SMES across multiple lines. Connecting a single SMES to multiple traction lines enables independent energy exchange for any line requiring compensation, as shown in Figure 6. Specifically, when two or more traction lines simultaneously require compensation, the SMES coils can be selectively controlled based on line priority to compensate the preferred line first.

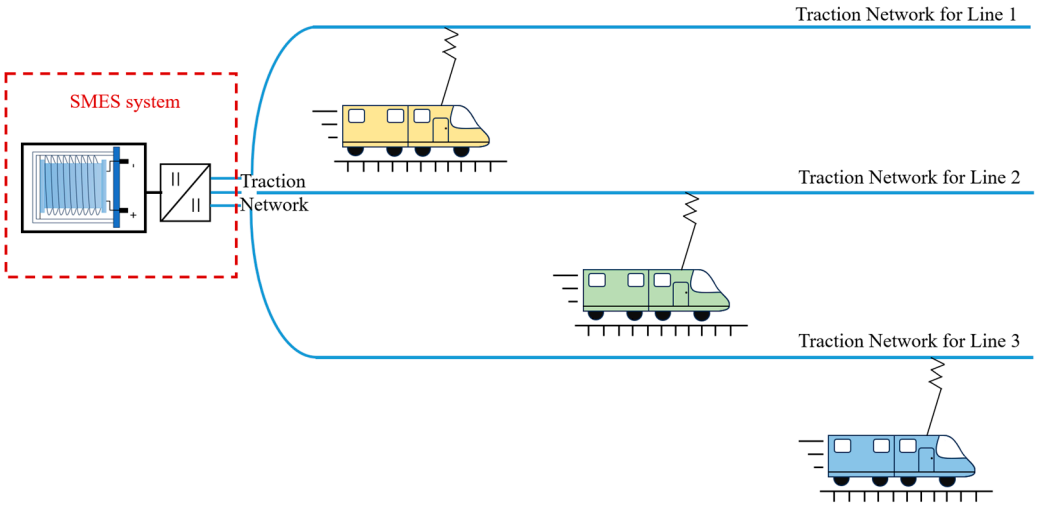

Figure 6. Schematic of SMES for multi-line configuration.

Considering that train operations involve starting conditions causing line voltage drops and regenerative braking conditions causing voltage surges, coupled with the current rail transit traction system's relatively single power source and poor risk resistance, significant voltage spikes can rapidly occur within subway stations when multiple trains perform regenerative braking simultaneously. These surges exceed specified limits, compromising train operational safety. Therefore, building upon the single-line simulation experiments described above, this study investigates cooperative control methods and simulation verification for scenarios involving multi-line mixed operation (including various states such as starting, regenerative braking, and constant-speed operation) when only a single superconducting energy storage system is deployed within a subway station. The goal is to establish a simulation platform that more closely approximates actual subway operating conditions, thereby advancing the application research of superconducting energy storage systems within subway station DC power supply systems.

4.3.1. Different Scenarios of Multi-Line Operation

In large subway stations with multiple lines, while each line could be equipped with a separate superconducting energy storage device to enhance power supply stability, current research trends favor increasing the capacity of individual SMES units due to the high cost of SMES equipment, the requirement for cryogenic operating environments, and significant long-term maintenance expenses. Therefore, the concept involved equipping large subway

stations with a single, high-capacity SMES unit to supply multiple lines. However, when multiple lines simultaneously require power, resource allocation conflicts arise. Although SMES offers millisecond-level response capability, its instantaneous output capacity was limited, necessitating prioritization of the most critical line. To address this, given the varying importance of different lines within a station, priority levels must be assigned to lines converging at the same station.

Matlab Simulink was employed to model and simulate a scenario where a single superconducting energy storage system serves three lines. For this simulation experiment, line importance was set as: Line 1 > Line 2 > Line 3. The experimental design utilized the Matlab function module within the software, implementing a three-tier priority voltage control system via code. Its core control philosophy is: the control system consistently regulates the voltages of Lines 1, 2, and 3 according to the absolute priority sequence V1, V2, V3, while incorporating a 10 V tolerance to prevent the controller from repeatedly switching between "charging" and "discharging" states during minor fluctuations near the nominal voltage value. V2, V3 in absolute priority order while maintaining a 10 V tolerance. This prevents the controller from repeatedly switching between "charge" and "discharge" states during minor fluctuations near the nominal voltage, which would cause frequent IGBT/Diode switching, increasing losses and heat generation. Additionally, actual voltage measurements may contain noise or minor fluctuations; the tolerance filters out these disturbances to prevent false actions. Only after the voltage of a high-priority line stabilizes within the tolerance range of 1500 V $\pm$ 10 V will switching to process a lower-priority line be permitted.

During each control cycle, the system first checks whether the target line's voltage has entered the tolerance range. If the voltage falls between 1490 V and 1510 V, the line is marked as processed. Subsequently, when no current target exists, the system checks the voltage fluctuations of subsequent lines in priority order. If a high-priority line is detected to have fluctuations exceeding the tolerance range—such as falling below 1490 V or rising above 1510 V—control is immediately preempted for handling. Only when all higher-priority lines are in a stable state will fluctuations on lower-priority lines be addressed. This design ensures that voltage regulation for high-priority lines always receives immediate response, while adjustments for lower-priority lines must wait until high-priority tasks are completed. This establishes a clearly hierarchical, orderly voltage regulation system that ultimately controls the multiplexer via output control signals to select the line requiring adjustment.

Considering that this paper simulates three lines, the simulation time was set to 5 s.

This simulation continued to validate the suppression effect of superconducting energy storage devices on voltage fluctuations in subway station traction systems through comparative simulation analysis. The subsequent simulation results presented voltage waveform changes with and without SMES integration. By adjusting key parameters—including the sequence, amplitude, and duration of voltage fluctuations across different lines, as well as the initial current of the energy storage magnets—we examined SMES's dynamic response characteristics and voltage stabilization performance under various conditions. This enables a comprehensive evaluation of its contribution to enhancing grid stability during actual operation.

Scenario ①: At 0.5 s, Line 1 voltage rose to 1600 V and fluctuated for 1 s. At 2 s, Line 2 voltage rose to 1700 V and fluctuated for 1 s. At 3.5 s, Line 3 voltage rose to 1800 V and fluctuated for 1 s. The initial current of the energy storage magnet was 500 A.

Comparing simulation results in Figure 7 revealed that the fluctuation of the traction system voltage was significantly suppressed after configuring the SMES system. According to the established control strategy, the superconducting energy storage system first

suppressed voltage fluctuations on V1, then on V2, and finally on V3. For fluctuations on Line 2 and Line 3, the SMES responds rapidly, effectively absorbing electrical energy to dampen voltage fluctuations. Although Line 3 experienced voltage spikes at specific time points, the amplitude of voltage fluctuations was significantly reduced, with peak voltage fluctuations capped at 1590 V and a swift return to the stable range. Due to capacity limitations of the superconducting energy storage device and the greater magnitude of Line 3's voltage fluctuations, the device could not fully suppress its voltage variations. Overall, the superconducting energy storage system demonstrated excellent dynamic regulation capabilities during multi-line, multi-time-point voltage disturbances.

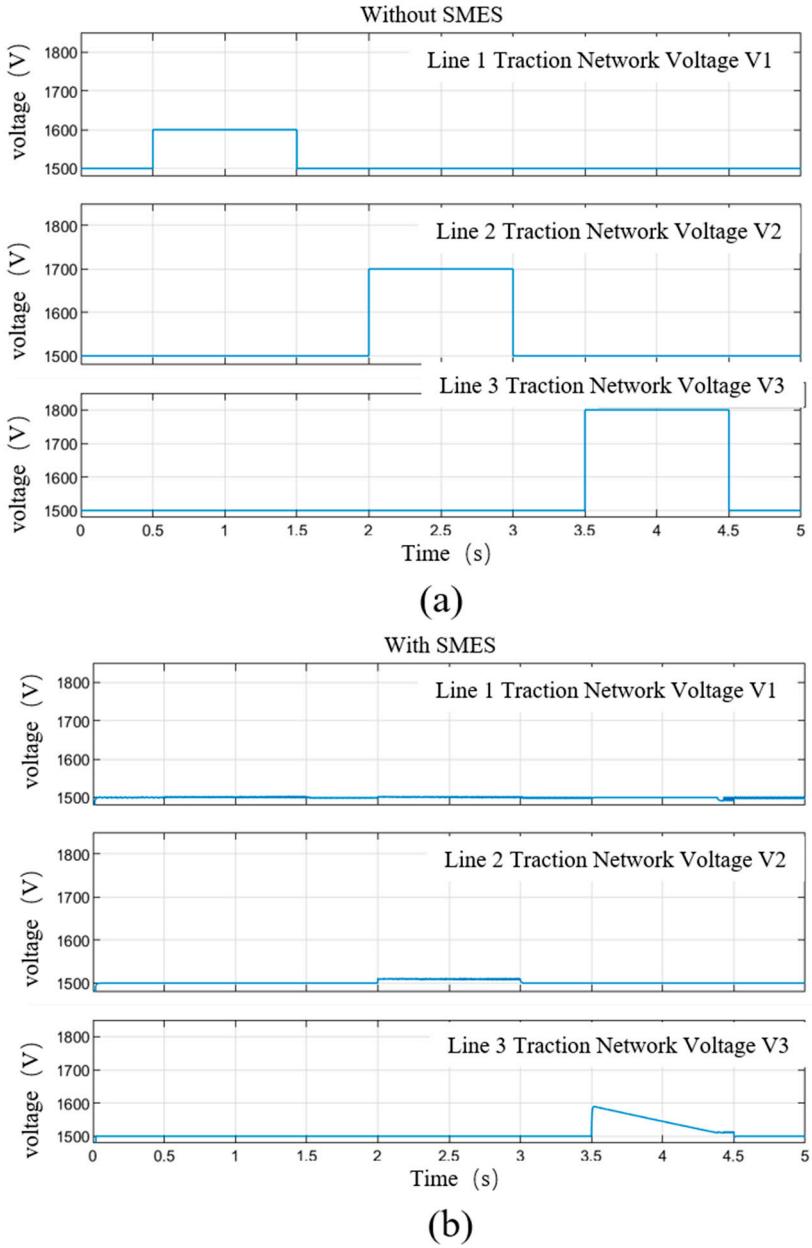

Figure 7. Scenario ①: (**a**) without SMES, (**b**) with SMES.

Scenario ②: At nearly simultaneous time 1 s, it caused Line 1 voltage to rise to 1600 V and fluctuate continuously for 0.5 s, caused Line 2 voltage to rise to 1700 V and fluctuate continuously for 1.25 s, and caused Line 3 voltage to rise to 1800 V and fluctuate continuously for 3.25 s.

As shown in simulation results Figure 8, under Scenario 3 without SMES configuration, voltage surges (1600 V, 1700 V, 1800 V) from Line 1, Line 2, and Line 3 occur nearly simultaneously at 1 s. When SMES was configured, the control strategy prioritizes V1 > V2 > V3. After Line 1 voltage V1 reaches its nominal value, it then suppressed voltage fluctuations on Line 2 voltage V2. Once both V1 and V2 reach their nominal values, it finally suppressed voltage fluctuations on Line 3.

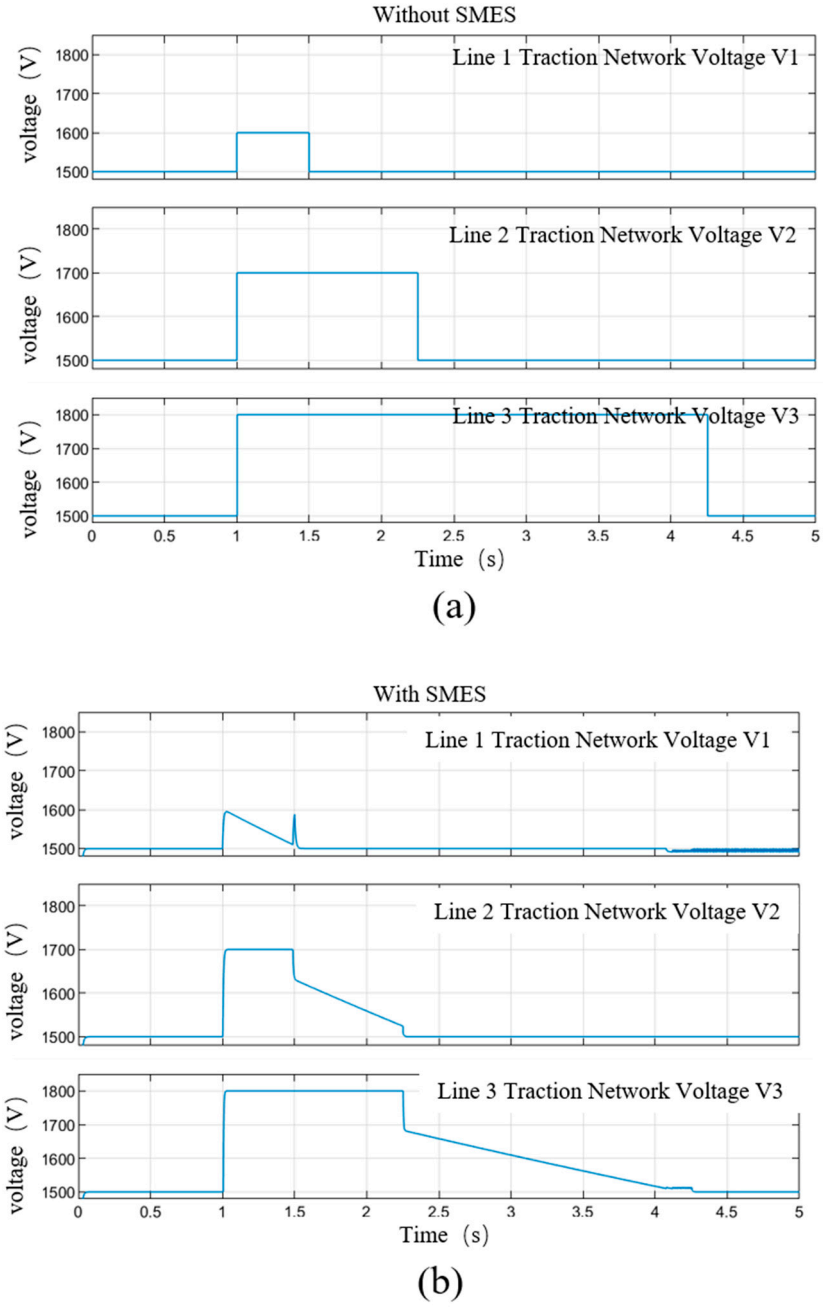

Figure 8. Scenario ②: (**a**) without SMES (**b**) with SMES.

Scenario ③: At 0.1 s, reduced Line 3 voltage to 1400 V and maintained for 1 s. At 2 s, reduced Line 2 voltage to 1400 V and maintained for 1 s. At 3.5 s, reduced Line 1 voltage to 1400 V and maintained for 1 s. The initial current of the energy storage magnet was 500 A.

As shown in Figure 9 and Table 2, under Scenario 3, without the SMES configured, the voltages dropped to 1400 V as impacted by lines 3, 2, and 1 at 0.1 s, 2 s, and 3.5 s, respectively. With SMES configured, following the configured control strategy, the SMES

first released energy to compensate for V3, then compensate for V2, and finally compensate for V1. The simulation results showed that the voltage fluctuations on lines 2 and 3 are completely suppressed. The 600 A case could fully compensate for the voltage drop within a short time. However, the 500 A case could not fully compensate for the voltage drop.

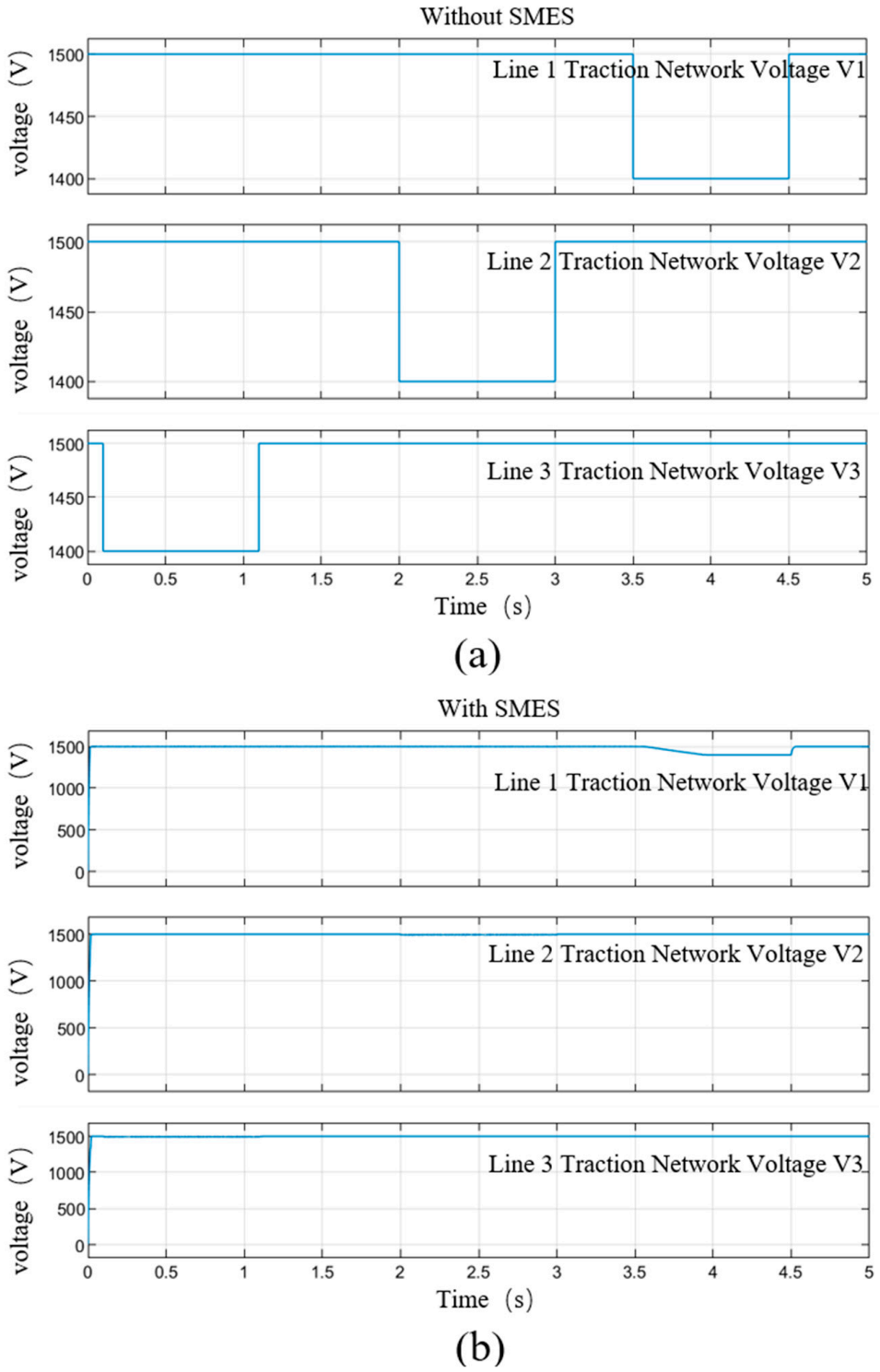

Figure 9. *Cont.*

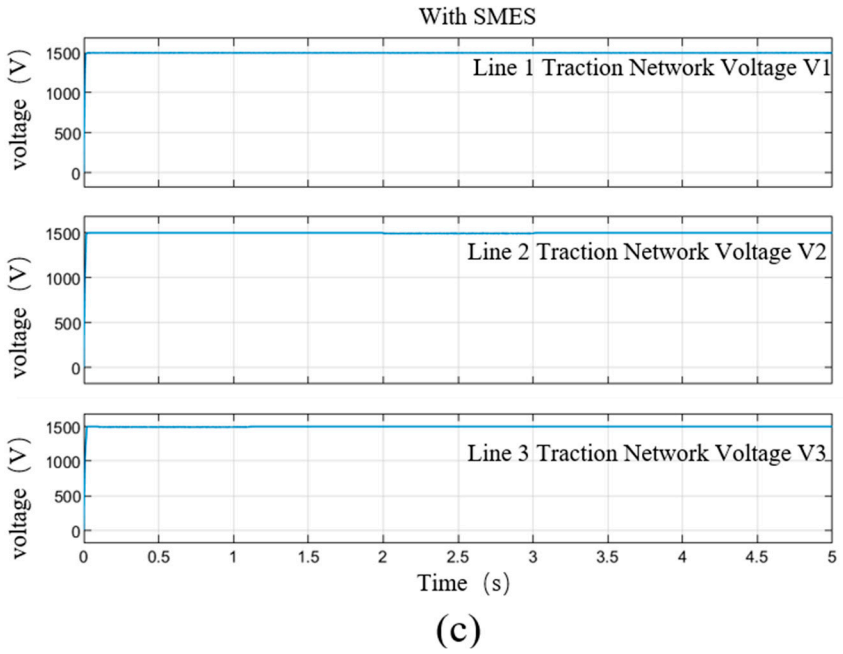

Figure 9. Scenario ③: (**a**) without SMES (**b**) with SMES, at an initial current of 500 A (**c**) with SMES, at an initial current of 600 A.

Table 2. Comparison of the SMES with initial currents at 500 A and 600 A, towards the maximum voltage fluctuation (Line 1).

Item	500 A	600 A
Maximum voltage fluctuation (Line 1)	6.667%	0.267%

4.3.2. Analysis

Simulation for the three scenarios above indicates that configuring a SMES system within the traction power supply system and implementing a three-tier priority voltage control strategy enabled effective suppression of voltage fluctuations and enhanced grid stability. The SMES regulated in the sequence V1, V2, V3, ensuring voltage fluctuations on high-priority lines were suppressed first. Only after the voltage on high-priority lines returns to nominal values were fluctuations on lower-priority lines addressed. In Scenario 1, the fluctuation on V1 was first suppressed to its nominal value, followed by sequential handling of V2 and V3. In Scenario 2, where all three lines fluctuate nearly simultaneously, the SMES prioritized V1 first. Upon restoring V1 to nominal, it immediately addressed V2's fluctuation and then proceeded to V3. The SMES rapidly responded to voltage transients, significantly reducing both the amplitude and duration of fluctuations. In both Scenario 1 and Scenario 2, although line voltages rose to 1600 V and 1700 V, respectively, the SMES swiftly pulled them back near nominal values. In voltage sag scenarios like Scenario 3, the SMES compensated for voltage drops by releasing stored energy. However, due to energy storage capacity limitations, fluctuations on lower-priority lines—such as V1 in Scenario 3—were not fully mitigated. This indicated that the SMES's energy storage capacity required further optimization to accommodate more severe scenarios. Thus, the SMES control system demonstrated robust voltage suppression capabilities across various disturbance scenarios. However, for suppressing complex voltage fluctuations across multiple lines and time points, further integration with energy storage capacity optimization was required to enhance its capability in handling extreme operating conditions.

5. Conclusions

This paper proposed a novel voltage compensation method utilizing SMES to suppress voltage fluctuations in the traction system of a large subway station with multiple lines. An SMES compensation system was employed to enhance power quality for subway trains, ensuring stable power supply during operation. Using the MATLAB/Simulink platform, a model of the 1500 V DC traction network and SMES was constructed to validate the feasibility and superiority of SMES in suppressing voltage fluctuations and recovering regenerative braking energy.

One SMES for one line enabled rapid voltage compensation for the acceleration and regenerative braking, achieving millisecond-level response. When a single SMES was shared among multiple lines, the voltage fluctuation amplitude decreased to 0.267%. To address energy allocation conflicts, this paper proposed a priority sequence for lines converging at the same subway station. Simulation shows that one SMES device was configured for three lines, and a three-level priority voltage control strategy was used, and the system could suppress voltage fluctuations and enhance grid stability.

Future work will validate simulation results through experiments to further confirm the model's reliability and accuracy under actual operating conditions. In summary, SMES with the novel control strategies can offer a viable solution for addressing traction network power quality issues in large subway stations with multiple lines.

Author Contributions: Conceptualization, W.M., B.S. and L.F.; methodology, W.M., B.S. and X.C.; software, W.M. and Y.C.; validation, W.M., B.S. and X.C.; writing—original draft preparation, W.M. and B.S.; writing—review and editing, B.S., X.C. and L.F.; supervision, B.S. and L.F.; project administration, B.S. All authors have read and agreed to the published version of the manuscript.

Funding: This work was supported in part by the National Natural Science Foundation of China under Grant No. 52472382, and the Fundamental Research Funds for the Central Universities.

Data Availability Statement: The data presented in this study are available on request from the corresponding author.

Conflicts of Interest: The authors declare no conflicts of interest.

References

1. Bi, Z.; Guo, R.; Khan, R. Renewable Adoption, Energy Reliance, and CO_2 Emissions: A Comparison of Developed and Developing Economies. *Energies* **2024**, *17*, 3111. [CrossRef]
2. Gómez, J.; Castro, R. Green Hydrogen Energy Systems: A Review on Their Contribution to a Renewable Energy System. *Energies* **2024**, *17*, 3110. [CrossRef]
3. Adetokun, B.B.; Oghorada, O.; Abubakar, S.J. Superconducting magnetic energy storage systems: Prospects and challenges for renewable energy applications. *J. Energy Storage* **2022**, *55*, 105663. [CrossRef]
4. Arsénio Costa, A.J.; Morais, H. Power Quality Control Using Superconducting Magnetic Energy Storage in Power Systems with High Penetration of Renewables: A Review of Systems and Applications. *Energies* **2024**, *17*, 6028. [CrossRef]
5. Chen, Y.; Fu, L.; Chen, X.; Jiang, S.; Chen, X.; Xu, J.; Shen, B. Ultra-low electrical loss superconducting cables for railway transportation: Technical, economic, and environmental analysis. *J. Clean. Prod.* **2024**, *445*, 141310. [CrossRef]
6. Wu, D.; Chau, K.T.; Liu, C.; Gao, S.; Li, F. Transient stability analysis of SMES for smart grid with vehicle-to-grid operation. *IEEE Trans. Appl. Supercond.* **2011**, *22*, 5701105.
7. Alkhafaji, A.S.; Trabelsi, H. Uses of Superconducting Magnetic Energy Storage Systems in Microgrids under Unbalanced Inductive Loads and Partial Shading Conditions. *Energies* **2022**, *15*, 8597. [CrossRef]
8. Guo, W.; Hong, Y.; Lan, J.; Yang, Y. Multi-Functional Device Based on Superconducting Magnetic Energy Storage. *Energies* **2024**, *17*, 3175. [CrossRef]
9. Boom, R.W.; Peterson, H.A. Superconductive energy storage for power systems. *IEEE Trans. Magn.* **1972**, *8*, 701–703. [CrossRef]
10. Boenig, H.J.; Hauer, J.F. Commissioning tests of the Bonneville power administration 30 MJ superconducting magnetic energy storage unit. *IEEE Power Eng. Rev.* **1985**, *104*, 302–312.

11. Guo, S. Research on the Ring-Shaped High-Temperature Superconducting Energy Storage Magnet's State Assessment Method. Ph.D. Thesis, Huazhong University of Science and Technology, Wuhan, China, 2022.
12. Guo, W.; Zhang, J.; Zhang, Z.; Qiu, Q.; Zhang, G.; Lin, L.; Xiao, L. Current research status and application prospect of SMES. *Sci. Technol. Rev.* **2016**, *34*, 68–80.
13. Gao, Y. Structural Design and Research on Thermal Stability of 10 MJ HTS SMES. Master's Thesis, North China Electric Power University, Beijing, China, 2023.
14. Ishigaki, Y.; Shirahama, H.; Kuroda, K. Power control experiments using a 5 MJ superconducting magnetic energy storage system. In Proceedings of the PESC'88 Record, 19th Annual IEEE Power Electronics Specialists Conference, Kyoto, Japan, 11–14 April 1988.
15. Honma, H.; Fujibayashi, K.; Asano, K.; Endo, M. Development of a 1 MJ SMES with quench enthalpy protection. *IEEE Trans. Energy Convers.* **1993**, *83*, 442–447. [CrossRef]
16. Kim, H.J.; Seong, K.C.; Cho, J.W.; Bae, J.H.; Sim, K.D.; Kim, S. 3 MJ/750 kVA SMES System for Improving Power Quality. *IEEE Trans. Appl. Supercond.* **2006**, *16*, 574–577. [CrossRef]
17. Fang, J.; Wen, J.; Wang, S.; Shi, J.; Ren, L.; Tang, Y.; Peng, X. Development and test of moveable conduction-cooled high-temperature superconducting magnetic energy storage system. *CSEE J. Power Energy Syst.* **2011**, *31*, 169–174.
18. Song, M.; Shi, J.; Liu, Y.; Xu, Y.; Hu, N.; Tang, Y.; Ren, L.; Li, J. 100 kJ/50 kW HTS SMES for Micro-Grid. *IEEE Trans. Appl. Supercond.* **2015**, *25*, 5700506. [CrossRef]
19. Suzuki, S.; Baba, J.; Shutoh, K.; Masada, E. Effective application of superconducting magnetic energy storage (SMES) to load leveling for high speed transportation system. *IEEE Trans. Appl. Supercond.* **2004**, *14*, 713–716. [CrossRef]
20. Dai, S.; Wang, B.; Ma, T. Superconducting magnetic energy storage system: Status and prospect. *Electr. Power Constr.* **2016**, *37*, 18–23.
21. Song, M.; Zou, X.; Ma, T.; Li, L.; Long, F.; Xu, Y. Overall design of a 5 MW/10 MJ hybrid high-temperature superconducting energy storage magnets cooled by liquid hydrogen. *Supercond. Sci. Technol.* **2024**, *37*, 025003. [CrossRef]
22. Chen, Y.; Chen, X.; Fu, L.; Jiang, S.; Shen, B. Superconducting hydrogen-electricity multi-energy system for transportation hubs: Modeling, technical study and economic-environmental assessment. *Appl. Energy* **2025**, *401*, 126823. [CrossRef]
23. Chen, X.; Xie, Q.; Bian, X.; Shen, B. Energy-saving Superconducting Magnetic Energy Storage (SMES) Based Interline DC Dynamic Voltage Restorer. *CSEE J. Power Energy Syst.* **2022**, *8*, 238–248.
24. Dong, H.; Tian, Z.; Spencer, J.; Fletcher, D.; Hajiabady, S. Coordinated control strategy of railway multisource traction system with energy storage and renewable energy. *IEEE Trans. Intell. Transp. Syst.* **2023**, *24*, 15702–15713. [CrossRef]
25. Ceraolo, M.; Lutzemberger, G.; Meli, E.; Pugi, L.; Rindi, A.; Pancari, G. Energy storage systems to exploit regenerative braking in DC railway systems: Different approaches to improve efficiency of modern high-speed trains. *J. Energy Storage* **2018**, *16*, 269–279. [CrossRef]
26. Xuan, Y. The Strategy of Multiphase Interleaved Bi-Directional DC-DC Converter for Absorbing the Regenerating Energy in Metro-Transit Systems. Master's Thesis, Southwest Jiaotong University, Chengdu, China, 2023.
27. Yang, Z. Analysis of the Impact of Voltage Fluctuations on Subway Equipment from the State Grid Side and Countermeasures. *Mech. Electr. Inf.* **2025**, *9*, 17–19.
28. Yan, S. On the solution to the problem of anti-voltage fluctuation of subway elevator power supply. *Autom. Appl.* **2021**, *4*, 104–108. [CrossRef]
29. Zhang, J.; Zhang, N.; Ge, Y. Energy storage placements for renewable energy fluctuations: A practical study. *IEEE Trans. Power Syst.* **2022**, *38*, 4916–4927. [CrossRef]
30. Cheng, P.; Kong, H.; Ma, J.; Jia, L. Overview of resilient traction power supply systems in railways with interconnected microgrid. *CSEE J. Power Energy Syst.* **2021**, *7*, 1122–1132.
31. Bade, S.K.; Kulkarni, V.A. Analysis of Railway Traction Power System Using Renewable Energy: A Review. In Proceedings of the 2018 International Conference on Computation of Power, Energy, Information and Communication (ICCPEIC), Chennai, India, 28–29 March 2018.
32. Fu, L.; Chen, Y.; Zhang, M.; Chen, X.; Shen, B. Multifunctional superconducting magnetic energy compensation for the traction power system of high-speed maglevs. *Electronics* **2024**, *13*, 979. [CrossRef]
33. Shen, B.; Chen, Y.; Xu, J.; Wang, W.; Lin, G.; Chen, X.; Fu, L. Superconducting Magnetic Energy Storage (SMES) for Urban Railway Transportation. *IEEE Trans. Appl. Supercond.* **2024**, *34*, 5701304. [CrossRef]
34. Meng, J. Study on Energy Consumption Analysis and Energy Saving Forecast of Ventilation and Air Conditioning System in Subway Station. Master's Thesis, Hebei University of Architecture, Zhangjiakou, China, 2020.
35. Xun, J.; Zhang, J.; Sun, Y.; Wu, Y. Pattern recognition of electrical energy for urban rail transit by using data mining. *J. Beijing Jiaotong Univ.* **2020**, *44*, 8–16.
36. Zhen, Y. Research on Power Lighting Systems for Subway Stations. *Sci. Technol. Innov. Inf.* **2018**, *1*, 82–83.

37. Zhang, R. Research on Regenerating Energy Utilization Technique in Urban Rail System. Master's Thesis, Beijing Jiaotong University, Beijing, China, 2012.
38. Chen, X.; Zhang, M.; Jiang, S.; Gou, H.; Zhou, P.; Yang, R.; Shen, B. Energy reliability enhancement of a data center/wind hybrid DC network using super-conducting magnetic energy storage. *Energy* **2023**, *263*, 125622. [CrossRef]
39. *GB/T 1402-2010*; Railway Applications. Supply Voltages of Traction Systems. State General Administration of the People's Republic of China for Quality Supervision and Inspection and Quaran-tine: Beijing, China; National Standardization Administration: Beijing, China, 2011.
40. Wu, D. Research on Photovoltaic Grid-Connected Low-Voltage Ride-Through Based on Superconducting Magnetic Energy Storage. Master's Thesis, Hunan University, Changsha, China, 2021.

Disclaimer/Publisher's Note: The statements, opinions and data contained in all publications are solely those of the individual author(s) and contributor(s) and not of MDPI and/or the editor(s). MDPI and/or the editor(s) disclaim responsibility for any injury to people or property resulting from any ideas, methods, instructions or products referred to in the content.